International Journal of Engineering & Technology, 7 (4.10) (2018) 613-618

International Journal of Engineering & Technology

Website: www.sciencepubco.com/index.php/IJET

Research paper

3D- flow of a Electrically Conducting and Dissipating Maxwell fluid treated with Ohmic Heating Convective boundary condition: Numerical Analysis

B.Malliswari[1], P.Sreenivasulu[2], T.Poornima[3]* and N.Bhaskar Reddy[1]

[1,4]Department of Mathematics, Sri Venkateswara University, Tirupati, A.P.-517502, India.
[2]Department of Mathematics, Sri Venkateswara College of Engineering for Women, Tirupati, A.P.-517502, India.
[3]Department of SAS, VIT University, Vellore, T.N.-632014, India.
**Corresponding author E-mail: poornima.t@vit.ac.in*

Abstract

An analysis is made to study the effects of radiation, dissipation, Thermo-diffuso and Diffuso- thermo on MHD 3D Maxwell flow past a stretching permeable sheet with resistive heating. Transforming the governing dimensional boundary layer equations using three dimensional similarity transformations and then the resultant equations are numerically solved by employing Shooting method. The effect of the pertinent parameters on various flow distributions is elaborately discussed with the help of graphs and tables. The comparison of present results with the existing literature gave an excellent agreement for the reduced cases.

Keywords: *Convective boundary condition; Dissipation; Joule heating; Maxwell fluid; MHD; Radiation, Stretching sheet.*

1. Introduction

The flow of non-Newtonian fluids received the attention of global investigators by its special, unique behaviour and novel applications. Some of the industrious processes such as plastic material production, chemical and petroleum industries, paints production uses this type of new fluid as it involves the properties of rheological liquids. Abbas *et al.*[1] studied the impact of thermal transfer on Maxwell fluid flow past an exponential stretching sheet. Numerous works found on Maxwell fluid past different geometries [2-5].

Non-Newtonian fluids with Magnetohydrodynamic along extending sheet have its enormous applications in nuclear reactors, plasma studies, polymer extraction. Palani *et al.* [6] investigated the chemical reaction effect on unsteady MHD flow of an UCM fluid past stretching sheet. Bataller [7] discussed heat transfer influence on UCM fluid over a stretching sheet. Shateyi [8] investigated the chemical reaction and thermophoresis effects on MHD Maxwell fluid over a vertical stretching sheet. Sreenivasulu *et al.* [9] investigated the effect of viscous dissipation and radiation on steady MHD Marangoni convection flow past a permeable flat plate in the presence of heat generation/ absorption. Kumari and Nath [10] investigated the mixed convection flow of Maxwell fluid past an exponential stretching vertical surface with MHD and dissipation. Bhaskar Reddy *et al.* [11] analysed the radiative heat transfer on MHD slip flow of dissipating Nano fluid over an exponential porous stretching sheet. Madhu *et al.*[12] evaluated the effect of radiation on MHD unsteady flow of Maxwell nanofluid past a stretching surface.

The flow subject to convective heat transfer have gained much interest among the researchers. Hayat *et al.*[13] presented the Soret and Dufour effects in three dimensional flow of Maxwell fluid in the presence of convective condition and chemical reaction. Yu Bai [14] presented the numerical analysis of fractional MHD Maxwell fluid with the effect of convective heat transfer condition and dissipation.

2. Transport Equations

Consider a steady, three dimensional radiating Maxwell flow past a non-linear elongating porous sheet with convective surface boundary condition. The sheet is stretched along the coordinate axes with the non-uniform velocities where a, b > 0. A transverse magnetic field of strength B_0 is applied in the direction perpendicular to the fluid flow. It is assumed that the sheet is stretched along the xy-plane, The sheet moves with the non-uniform velocities $u = u_w = ax,\ v = v_w = by$ where $a,\ b > 0$, along x and y directions respectively as shown in Fig. 1.

Additionally Soret and Dufour, viscous dissipation and resistive heating effects are also considered. Under the usual assumptions, the flow field equations are given below:

$$\frac{\partial u}{\partial x} + \frac{\partial v}{\partial y} + \frac{\partial w}{\partial z} = 0 \qquad (1)$$

3. Results and Discussion

In order to get the physical interpretation of the study the graphs and tables for different parameters are exhibited and discussed elaborately.

The effect of porosity parameter K on axial velocity, transverse velocity and temperature are respectively depicted in Figs. 2, 3 and 4. Similar to magnetic field parameter M, an increase in the porosity parameter K results the axial velocity and the transverse

velocity of the fluid decreases. Exactly the opposite behaviour is observed in case of temperature i.e. the temperature of the fluid decreases with an increase in the porosity parameter *K*.

$$u\frac{\partial u}{\partial x}+v\frac{\partial u}{\partial y}+w\frac{\partial u}{\partial z}=\nu\frac{\partial^2 u}{\partial z^2}+g\beta_T(T-T_\infty)+g\beta_c(C-C_\infty)-\frac{\sigma B_0^{\,2}}{\rho}u-\frac{\nu}{k_1}u \\ -\lambda\left(u^2\frac{\partial^2 u}{\partial x^2}+v^2\frac{\partial^2 u}{\partial y^2}+w^2\frac{\partial^2 u}{\partial z^2}+2uv\frac{\partial^2 u}{\partial x\partial y}+2vw\frac{\partial^2 u}{\partial y\partial z}+2uw\frac{\partial^2 u}{\partial x\partial z}\right) \tag{2}$$

$$u\frac{\partial v}{\partial x}+v\frac{\partial v}{\partial y}+w\frac{\partial v}{\partial z}=\nu\frac{\partial^2 v}{\partial z^2}-\frac{\sigma B_0^{\,2}}{\rho}u-\frac{\nu}{k_1}u \\ -\lambda\left(u^2\frac{\partial^2 v}{\partial x^2}+v^2\frac{\partial^2 v}{\partial y^2}+w^2\frac{\partial^2 v}{\partial z^2}+2uv\frac{\partial^2 v}{\partial x\partial y}+2vw\frac{\partial^2 v}{\partial y\partial z}+2uw\frac{\partial^2 v}{\partial x\partial z}\right) \tag{3}$$

$$u\frac{\partial T}{\partial x}+v\frac{\partial T}{\partial y}+w\frac{\partial T}{\partial z}=\alpha\frac{\partial^2 T}{\partial z^2}-\frac{1}{\rho Cp}\frac{\partial q_r}{\partial z}+\frac{D_e k_T}{C_e C_p}\frac{\partial^2 C}{\partial z^2}+\frac{\sigma B_0^{\,2}}{\rho Cp}(u^2+v^2) \\ +\frac{\mu}{\rho Cp}\left[\left(\frac{\partial u}{\partial z}\right)^2+\left(\frac{\partial v}{\partial z}\right)^2\right]+\frac{\mu_f}{\rho Cp}\left[\left(\frac{\partial^2 u}{\partial z^2}\right)^2+\left(\frac{\partial^2 v}{\partial z^2}\right)^2\right] \tag{4}$$

$$u\frac{\partial C}{\partial x}+v\frac{\partial C}{\partial y}+w\frac{\partial C}{\partial z}=D_e\frac{\partial^2 C}{\partial z^2}+\frac{k_T D_e}{T_m}\frac{\partial^2 T}{\partial z^2}-k_r(C-C_\infty) \tag{5}$$

The appropriate boundary conditions are

$$u=u_w=ax,\quad v=v_w=by,\quad w=0,\quad -k^*\left(\frac{\partial T}{\partial z}\right)=h(T_f-T),\ -D\left(\frac{\partial C}{\partial z}\right)=h^*(C_f-C)\quad at\ \ z=0 \\ u\to 0,\quad v\to 0,\ T\to T_\infty,\ C\to C_\infty \qquad as\ \ z\to\infty \tag{6}$$

Using Rosseland approximation, q_r is described as

$$q_r=-\frac{4}{3}\frac{\sigma_s}{k_e}\frac{\partial T^4}{\partial y} \tag{7}$$

It should be noted that by Rosseland approximation, we limit our analysis to optically thick fluids. If the temperature differences within in the flow are sufficiently small, then equation (7) can be linearized by expanding T^4 into the Taylor series about T_∞ and neglecting higher order terms to take the form:

$$T^4\cong 4T_\infty^3T-3T_\infty^4 \tag{8}$$

In view of equations (7) and (8), equation (4) becomes

$$u\frac{\partial T}{\partial x}+v\frac{\partial T}{\partial y}+w\frac{\partial T}{\partial z}=\frac{k}{\rho Cp}\left(1+\frac{16\sigma_s T_\infty^3}{3k_e k}\right)\frac{\partial^2 T}{\partial z^2}+\frac{\tau D_e k_T}{C_e C_p}\frac{\partial^2 T}{\partial z^2}+\frac{\mu}{\rho Cp}\left[\left(\frac{\partial u}{\partial z}\right)^2+\left(\frac{\partial v}{\partial z}\right)^2\right] \\ +\frac{\mu_f}{\rho Cp}\left[\left(\frac{\partial^2 u}{\partial z^2}\right)^2+\left(\frac{\partial^2 v}{\partial z^2}\right)^2\right]+\frac{\sigma B_0^{\,2}}{\rho Cp}(u^2+v^2) \tag{9}$$

Introducing the following similarity transformations,

$$u=u_w=axf',\quad v=v_w=ayg',\quad \eta=\sqrt{\frac{a}{\nu}}z,\ \theta(\eta)=\frac{T-T_\infty}{T_f-T_\infty},\quad \phi(\eta)=\frac{C-C_\infty}{C_w-C_\infty}, \\ w=-\sqrt{a\nu}(f+g),\lambda=\frac{Gr_x}{\mathrm{Re}_x^2},Gr_x=\frac{g\beta_T(T_f-T_\infty)x^3}{\nu^2},N=\frac{\beta_c(C_w-C_\infty)}{\beta_T(T_f-T_\infty)},M=\frac{\sigma B_0^2}{\rho a}, \\ K=\frac{\nu}{k_1a^2},c=\frac{b}{a},\mathrm{Pr}=\frac{k}{\rho Cp},R=\frac{4\sigma_s T_\infty^3}{3k_e k},Du=\frac{D_e K_T}{C_e Cp\,\nu}\frac{(C_w-C_\infty)}{(T_f-T_\infty)},Sr=\frac{D_e K_T}{T_m\nu}\frac{(T_f-T_\infty)}{(C_w-C_\infty)}, \\ \mathrm{Re}_x=\frac{u_w x}{\nu},\mathrm{Re}_y=\frac{u_w y}{\nu},Ec_x=\frac{u_w^2}{Cp_f(T_f-T_\infty)},Ec_y=\frac{v_w^2}{Cp_f(T_f-T_\infty)},Sc=\frac{\nu}{D_B},\gamma_1=\frac{h}{k^*}\sqrt{\frac{\nu}{a}}, \\ \gamma_2=\frac{h^*}{D}\sqrt{\frac{\nu}{a}} \tag{10}$$

In view of equations (9)-(10), the governing equations (2), (3), (5) and (9) reduce to the dimensionless form:

$$f'''+(f+g)f''-f'^2+\beta\left[2(f+g)f'f''-(f+g)^2f'''\right]+\lambda(\theta+N\phi)-(\mathrm{K}+M)f'=0 \tag{11}$$

$$g'''+(f+g)\mathrm{g}''-g'^2\left[2(f+g)g'g''-(f+g)^2g''\right]-(\mathrm{K}+M)\mathrm{g}'=0 \tag{12}$$

$$\frac{1}{\mathrm{Pr}}\left(1+\frac{4}{3}R\right)\theta''+(f+g)\theta'+Du\phi''+2\left[Ec_x f''^2+\left(\frac{1}{c}\right)^2Ec_y g''^2\right]+M\left[Ec_x f'^2+\left(\frac{1}{c}\right)^2Ec_y g'^2\right]=0 \tag{13}$$

$$\phi''+Sc(f+g)\phi'+ScSr\theta''-ScKr\phi=0 \tag{14}$$

The corresponding boundary conditions are

$$f(0)=0,\quad f'(0)=1,\quad g(0)=0,\quad g'(0)=c,\quad \theta'(0)=-\gamma_1(1-\theta(0)),\quad \phi'(0)=-\gamma_2(1-\phi(0)) \\ f'(\infty)\to 0,\quad g'(\infty)\to 0,\quad \theta(\infty)\to 0,\quad \phi(\infty)\to 0 \tag{15}$$

Engineering quantities which of our interest in their non-dimensional form :

$$C_{fx}\,\mathrm{Re}_x^{1/2}=f''(0),\quad C_{fy}\,\mathrm{Re}_y^{1/2}=\mathrm{g}''(0),Nu_x\,\mathrm{Re}_x^{-1/2}=-\theta'(0),Sh_x\,\mathrm{Re}_x^{-1/2}=-\phi'(0) \tag{16}$$

The influence of Deborah number on the axial velocity and transverse velocity are shown in Figs. 5 and 6 respectively. From these figures it is found that, both the velocities of the fluid decreases with an increase in the Deborah number. At higher values of Deborah number dominated by the elasticity and demonstrating solid like behaviour, due to this fact the velocity of the fluid of the fluid decreases.

The influence of stretching ratio parameter *c* on the axial velocity, transverse velocity and temperature profiles is shown in Figs. 7,8 and 9 respectively. It is noticed that the axial velocity and temperature of the fluid decreases with an increase in the stretching ratio parameter *c* while the transverse velocity of the fluid increases. It is fact that, the pressure on the fluid flow increases with an increase in stretching ratio parameter, due to this reason the temperature of the fluid decreases. It is observed from this figure that the temperature of the fluid decreases near the surface and it shows the opposite behaviour for away from the plate with an increase in the radiation parameter *R* (Fig. 10).

The influence of Dufour number and Soret number on the temperature and concentration profiles is shown in Figs. 11-14 respectively. It is clear that, in both the cases the temperature of the fluid increases near the plate and decreases for away from the plate and the same behaviour exhibits in the concentration profiles.

Figs. 15 and 16 presents the temperature profiles for different values of Eckert number Ec_x and Ec_y respectively. From these graphs it is evident that the temperature of the fluid increases with an increase in the Eckert number in both the directions (i.e. Ec_x and Ec_y). it is fact that the production of heat becomes higher thereby increases the on Ec_x and Ec_y and the corresponding boundary layer thickness.

The effect of thermal Biot number γ_1 on temperature is shown in Figs. 17. Physically the Biot number is expressed as the convection at the surface of the body to the conduction within the surface of the body. It is evident that the temperature of the fluid decreases with the higher values of thermal Biot number. The opposite behaviour is noticed on the solutal Biot number γ_2 on concentration which is shown in Fig.18.

The variations of $f''(0)$ and $g''(0)$ which are proportional to the local skin friction coefficient in axial and transverse direction are shown in Table. 2 for different values Deborah number β, magnetic parameter *M*, permeability parameter *K*, concentration buoyancy number *N*, mixed convection parameter λ and stretching ratio parameter *c*. It is seen that the surface skin friction rate along the both *x* and *y*-directions decreases with an increase in Deborah number, magnetic parameter, permeability parameter and stretching ratio parameter. Also it is observed that the surface skin friction rate along the *x*-direction decreases while the skin friction rate along the *y*-direction shows n opposite behaviour with an increase in concentration buoyancy number. It is evident from Table. 2 that an increasing values of mixed convection parameter results the surface skin friction along x-direction and decreases the skin friction along *y*-direction. It is fact that an increase in the buoyancy effect in mixed convection flow leads to an acceleration of the

fluid flow, which increases the local skin friction factor along the *x*-direction.

The effects of various governing physical parameters on heat and mass transfer rates are shown in Table. 3. It is seen that the heat transfer rate decreases while the mass transfer rate increases with an increasing values of Deborah number. The effect of increasing the value of Pr is to decrease the heat transfer coefficient and increases the mass transfer coefficient. The effect of increasing the value of R is to increase the rate of heat transfer and decreases the mass transfer coefficient. Finally, the effects of Eckert number, chemical reaction parameter, convective boundary parameters, Dufour and Soret number on the rate of heat and mass transfers are shown in this table. The behavior of these parameters is self-evident from the Table.3 and hence is not discussed for brevity.

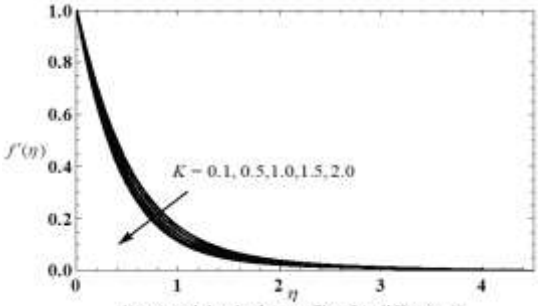

Fig.2 Axial velocity profiles for different K

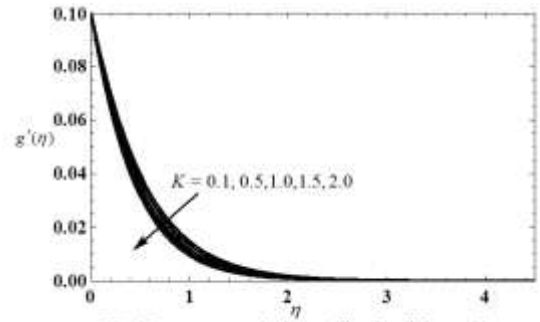

Fig.3 Transverse velocity profiles for different K

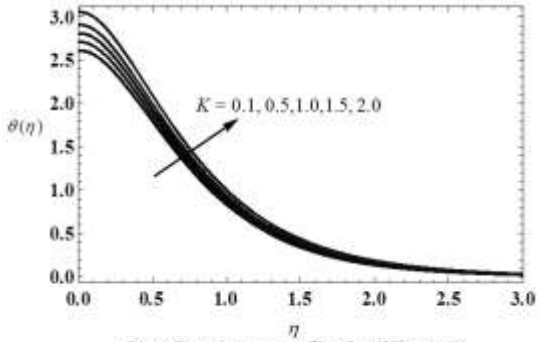

Fig.4 Temperature profiles for different K

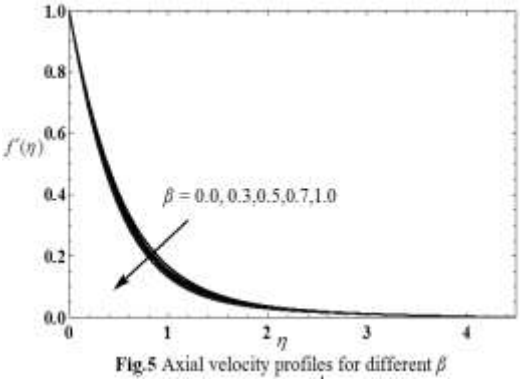

Fig.5 Axial velocity profiles for different β

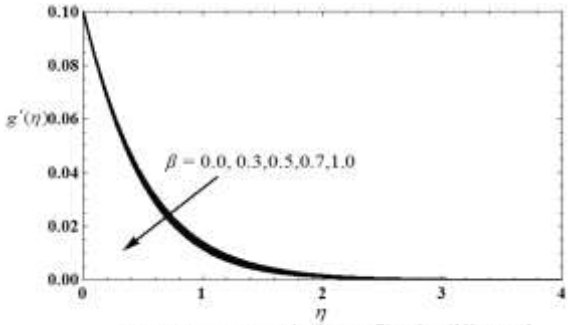

Fig.6 Transverse velocity profiles for different β

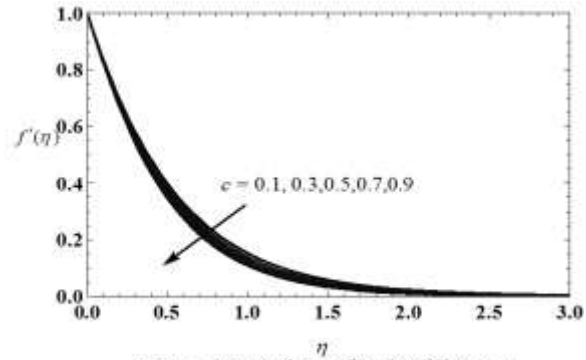

Fig.7 Axial velocity profiles for different c

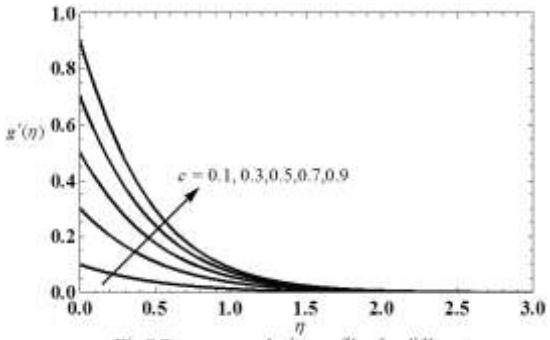

Fig.8 Transverse velocity profiles for different c

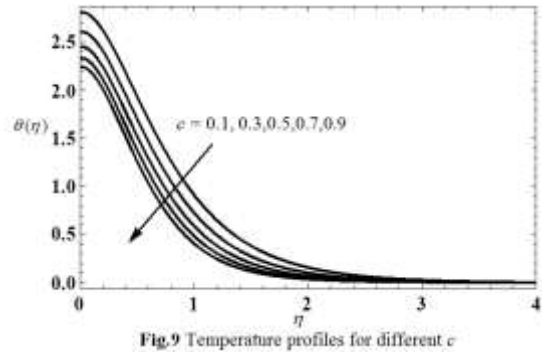

Fig.9 Temperature profiles for different c

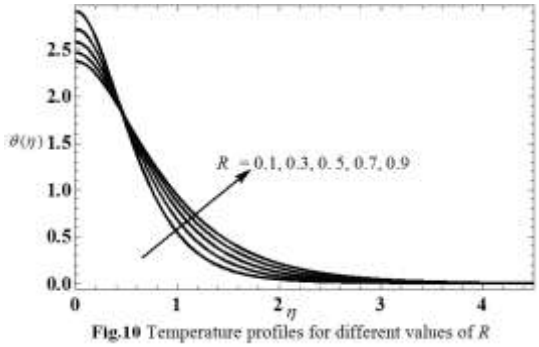

Fig.10 Temperature profiles for different values of R

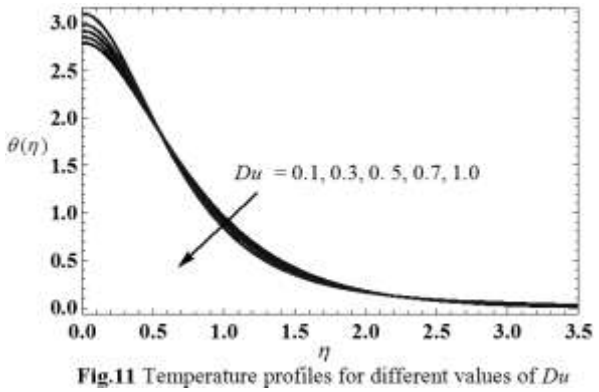

Fig.11 Temperature profiles for different values of *Du*

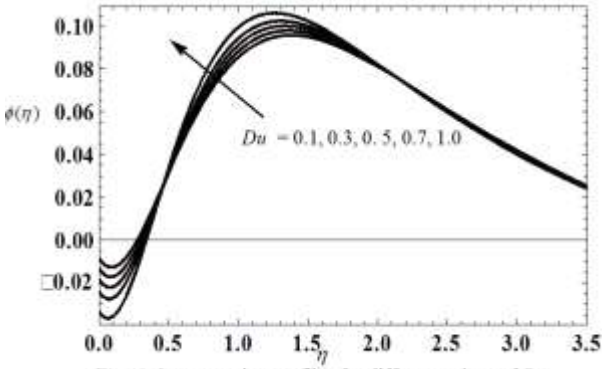

Fig.12 Concentration profiles for different values of *Du*

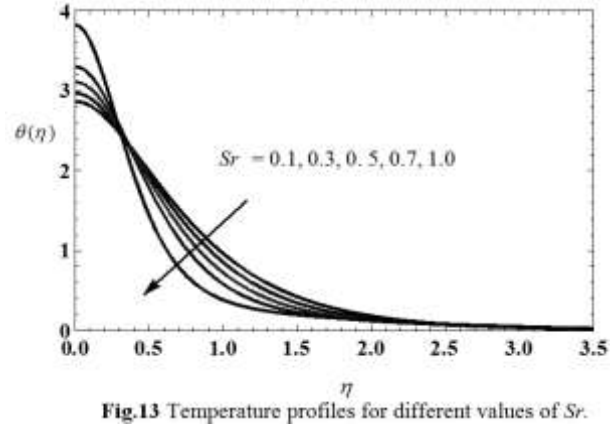

Fig.13 Temperature profiles for different values of *Sr*.

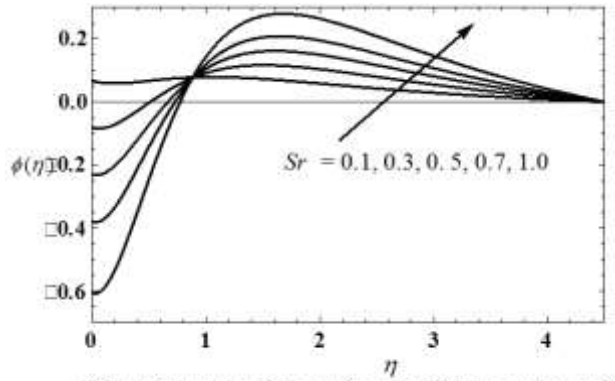

Fig.14 Concentration profiles for different values of *Sr*.

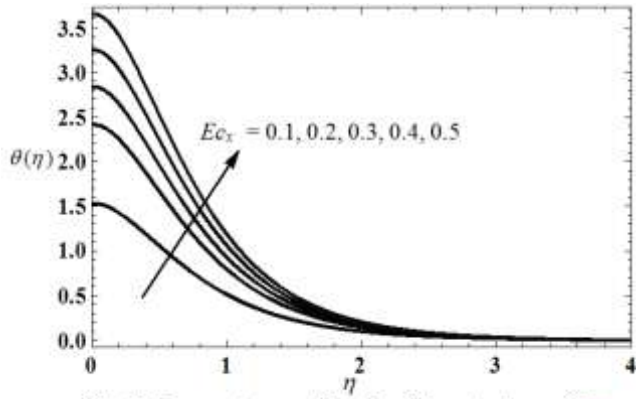

Fig.15 Temperature profiles for different values of Ec_x

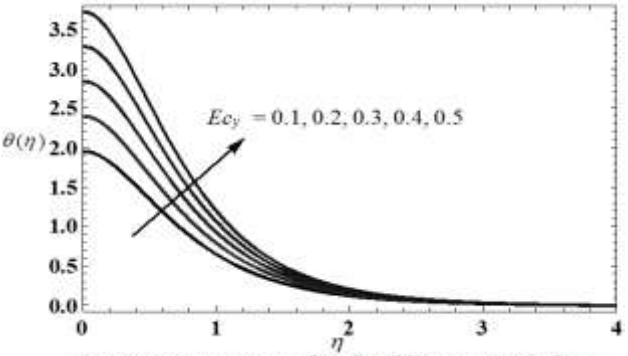

Fig.16 Temperature profiles for different values of Ec_y

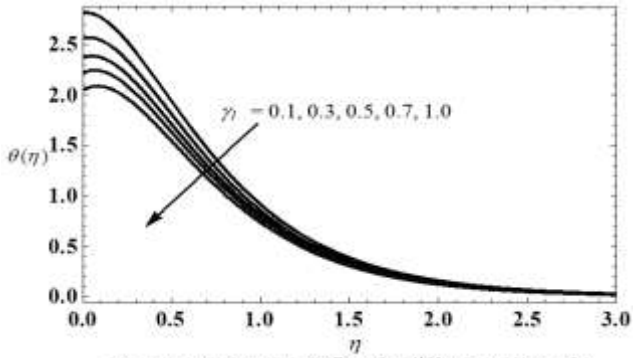

Fig.17 Temperature profiles for different values of γ_1

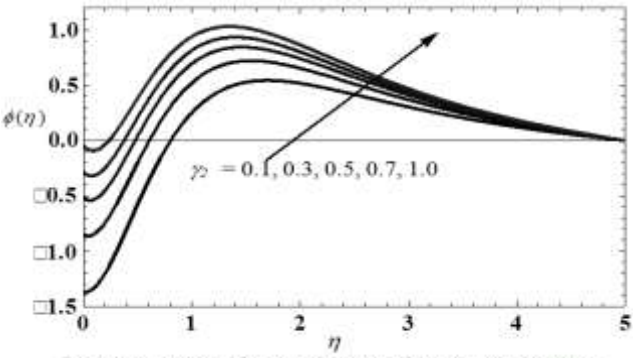

Fig.18 Concentration profiles for different values of γ_2

4. Conclusions

The present study gives numerical solutions for the effects of chemical reaction and convective surface boundary conditions on MHD three dimensional radiating flow of Maxwell fluid past a stretch sheet in the presence of Joule heating and viscous dissipation. Basing on the analysis, the following conclusion may be

drawn.The axial velocity of the fluid decreases with an increase in *M* or *K* or β and *c* but it increases with an increase in λ.

1. It is evident that the surface skin friction rate at the along *y*-direction increases with the higher values of N, but it decreases with an increase in *M* or *K* or β or λ and *c*.
2. The temperature of the fluid near the surface increases while it decreases for away from the plate with the higher values of *Du* or *Sr* and exactly the opposite behavior is noticed with an increase in *R*.

Table.1: comparison values of $-\theta'(0)$ for different values β, *c* and *Pr* for some reduced cases.

Pr	C	β	$-\theta'(0)$	
			Hayat *et al.*[15]	Present Study
0.7	0.5	0.4	0.282787	0.282342
1.2	0.5	0.4	0.340424	0.340243
1.6	0.5	0.4	0.368405	0.368123
2.0	0.5	0.4	0.388869	0.388764
1.0	0.0	0.4	0.287813	0.287345
1.0	0.4	0.4	0.316638	0.316543
1.0	0.7	0.4	0.330168	0.330234
1.0	1.0	0.4	0.340702	0.340654
1.0	0.5	0.0	0.330404	0.330245
1.0	0.5	0.3	0.321661	0.322348
1.0	0.5	0.8	0.308651	0.308321
1.0	0.5	1.2	0.299526	0.299041

Table.2: Values of $f''(0)$ and $g''(0)$ for different values β, *M*, *K*, λ and *c*.

β	*M*	*K*	*N*	λ	*C*	$f''(0)$	$g''(0)$
0.1	0.5	0.5	0.1	0.1	0.1	–1.78753	–0.18462
0.3						–1.81832	–0.18601
0.5						–1.84884	–0.18738
0.5	0.1					–1.74488	–0.17644
	0.5					–1.84884	–0.18738
	1.0					–1.97172	–0.20023
		0.1				–1.74192	–0.17646
		0.5				–1.84884	–0.18738
		1.0				–1.97475	–0.20021
			0.1			–1.74192	–0.17646
			0.5			–1.74734	–0.17644
			1.0			–1.75417	–0.17641
				0.1		–1.74192	–0.17646
				0.3		–1.61834	–0.17713
				0.5		–1.50736	–0.17775
					0.1	–1.74192	–0.17646
					0.3	–1.78442	–0.54337
					0.5	–1.82797	–0.93159

Table.3: Values of $-\theta'(0)$ and $-\phi'(0)$ for different values *M*, *Pr*, *R*, *Du*, Ec_x, Ec_y, *Sr*, *Kr*, γ_1 and γ_2

M	*Pr*	*R*	*Du*	Ec_x	Ec_y	*Sr*	*Kr*	γ_1	γ_2	$-\theta'(0)$	$-\phi'(0)$
0.1	0.7	0.5	0.3	0.3	0.3	0.2	0.5	0.1	0.1	–0.01801	0.09025
0.5										–0.03041	0.09075
1.0										–0.04505	0.09135
0.5	0.7									–0.03041	0.09075
	1									–0.05414	0.09199
	3									–0.12297	0.09681
		0.5								–0.03041	0.09075
		1.0								–0.00963	0.08974
		2.0								0.01385	0.08865
			0.1							–0.02914	0.09069
			0.3							–0.03041	0.09075
			0.5							–0.03166	0.09080
				0.1						0.00392	0.08922
				0.3						–0.03041	0.09075
				0.5						–0.06351	0.09221
					0.1					0.00461	0.08919
					0.3					–0.03041	0.09075
					0.5					–0.06525	0.09229
						0.1				–0.03023	0.08853

						0.3				–0.03057	0.09297
						0.5				–0.03092	0.09746
							0.1			–0.03006	0.08701
							0.3			–0.03027	0.08933
							0.5			–0.03041	0.09075
								0.1		–0.03041	0.09075
								0.3		–0.06376	0.09088
								0.5		–0.08167	0.09096
									0.1	–0.03041	0.09075
									0.3	–0.03257	0.21398
									0.5	–0.03398	0.29379

References

[1] Abbas Z, Javed T, Ali N, and Sajid M (2014), Flow and Heat Transfer of Maxwell Fluid Over an Exponentially Stretching Sheet: A Non-similar Solution. Heat Transfer-Asian Research, 43 (3).

[2] Mustafa M, Junaid Ahmad Khan, Hayat T, and Alsaedi A (2015), Simulations for Maxwell fluid flow past a convectively heated exponentially stretching sheet with nanoparticles. AIP Advances 5, 037133. https://doi.org/10.1063/1.4916364.

[3] Feng GAO and Xiao-Jun YANG (2016), Fractional Maxwell fluid with fractional derivative without singular kernel. Thermal Science 20(3), S871-S877.

[4] Josephe P (2017), Analysis of stagnation point flow of an upper-convected maxwell fluid. Electronic Journal of Differential Equations 2017(302),1–14.

[5] Azhar Ali Zafar, Muhammad Bilal Riaz and Muhammad Imran Asjad)(2018), Unsteady Rotational Flow of Fractional Maxwell Fluid in a Cylinder Subject to Shear Stress on the Boundary. Punjab University Journal of Mathematics 50(2), 21-32.

[6] Swati Mukhopadhyay and Krishnendu Bhattacharyya(2012), Unsteady flow of a Maxwell fluid over a stretching surface in presence of chemical reaction. Journal of the Egyptian Mathematical Society 20, 229–234.

[7] Sajid M, Abbas Z, Ali N, Javed T and Ahmad I(2014), Slip Flow of a Maxwell Fluid Past a Stretching Sheet. Walailak J Sci & Tech. 11(12), 1093-1103.

[8] Palani S, Rushi Kumar B and Kameswaran PK(2016), Unsteady MHD flow of an UCM fluid over a stretching surface with higher order chemical reaction. Ain Shams Engineering Journal 7, 399–408.

[9] Bataller RC (2011), Magnetohydrodynamic Flow and Heat Transfer of an Upper-Convected Maxwell Fluid Due to a Stretching Sheet. FDMP 7(2), 153-173.

[10] Shateyi S(2013), A new numerical approach to MHD flow of a Maxwell fluid past a vertical stretching sheet in the presence of thermophoresis and chemical reaction. Boundary Value Problems 2013,196.

[11] Sreenivasulu P, Poornima T and Bhaskar Reddy N (2017),Variable thermal conductivity influence on Hydromagnetic flow past a stretching cylinder in a thermally stratified medium with heat source/sink. Frontiers in Heat and Mass Transfer (FHMT) 9, 20. DOI: 10.5098/hmt.9.20.

[12] Kumari M and Nath G (2014), Mixed convection flow of Maxwell fluid over an exponentially stretching vertical surface with magnetic field and viscous dissipation.Meccanica 49(5), 1263–1274.

[13] Bhaskar Reddy N, Poornima T and Sreenivasulu P (2016), Radiative heat transfer effect on MHD slip flow of Dissipating Nanofluid past an exponential stretching porous sheet. International Journal of Pure and Applied Mathematics 109(9), 134 – 142.

[14] Madhu M, Kishana N , Chamkha AJ (2017), Unsteady flow of a Maxwell nanofluid over a stretching surface in the presence of magnetohydrodynamic and thermal radiation effects. Propulsion and Power Research 6(1),31–40.

[15] Hayat T, Ashraf MB, Alsaedi A, and Alhothuali MS (2015), Soret and Dufour effects in three-dimensional flow of Maxwell fluid with chemical reaction and convective condition. International Journal of Numerical Methods for Heat & Fluid Flow 25, 98–120. http://dx.doi.org/10.1108/HFF-11-2013-0322.

[16] Yu Bai, Yuehua Jiang, Fawang Liu, and Yan Zhang(2017), Numerical analysis of fractional MHD Maxwell fluid with the effects of convection heat transfer condition and viscous dissipation. AIP Advances 7, 125309.